SUPERCONDUCTING-STATE ENERGY GAP PARAMETERS FROM SPECIFIC HEAT MEASUREMENTS
MgB_2 and $Na_{0.3}CoO_2 \cdot 1.3H_2O$

N. E. Phillips[*] and R. A. Fisher

Department of Chemistry, University of California, and Lawrence Berkeley National Laboratory, Berkeley, CA 94720, USA

Specific heat data and their relation to the form of the energy gap are reviewed for Al, HfV_2, and two recently discovered superconductors, MgB_2 and $Na_{0.3}CoO_2 \cdot 1.3H_2O$. The data for Al and HfV_2 exemplify the specific heat of, respectively, weak- and strong-coupled BCS superconductors with isotropic energy gaps. MgB_2 is also known to be a BCS superconductor, but the specific heat deviates from BCS behavior in a way that shows the presence of two distinctly different energy gaps and characteristics of both weak and strong coupling. The heat capacity of $Na_{0.3}CoO_2 \cdot 1.3H_2O$ is strongly sample dependent, but suggests that it is another two-gap, possibly 'unconventional' superconductor.

Keywords: MgB_2, $Na_{0.3}CoO_2 \cdot 1.3H_2O$, specific heat, superconductors

Introduction

The thermodynamic properties of a superconductor are determined by the energy gap (Δ), its temperature (T) dependence, and its form in momentum space. In the superconducting-state, conduction-electron contribution to the specific heat (C_{es}) gives information about the form of the energy gap, the order parameter in the phenomenological theory, and, therefore, clues to the nature of the electron-pairing mechanism, which establishes the gap. In the BCS theory [1], the electron pairing is phonon mediated, and the gap is isotropic, spin-singlet, s-wave. In the weak-coupling limit, $\Delta(T)$ is a universal function of the reduced temperature, T/T_c, where T_c is the critical temperature, and $\Delta(0)/k_B T_c = 1.764$. C_{es} is an approximately exponential function of T/T_c. Data for Al [2] are shown in Fig. 1, where they are plotted in reduced form, as $C_{es}/\gamma T$, where γ is the coefficient of the conduction-electron specific heat (C_e) in the normal-state, where $C_e = C_{en} = \gamma T$. To within the precision of the measurements, they conform to the BCS theory in the weak-coupling limit.

In the theory for strong coupling, $\Delta(T)$ and the thermodynamic properties are no longer universal functions of the single parameter, T/T_c. However, the properties of strong-coupled superconductors have been very successfully represented by the α model [3], in which $\Delta(0)/k_B T_c \equiv \alpha$ is taken to be an adjustable parameter, instead of the constant, 1.764, of the weak-coupling theory, but the BCS temperature de-

pendence for $\Delta(T)$ is assumed. The α model gives all the thermodynamic properties, with thermodynamic consistency, as functions of α and T/T_c. HfV_2 has been thought to be an 'unconventional' superconductor because C_{es} shows the T^3 dependence expected for point nodes in the gap, but recent measurements [4] have shown that the reported T^3 dependence is really a manifestation of strong coupling, and, in the limit $T \rightarrow 0$, where the T^3 dependence would indicate point
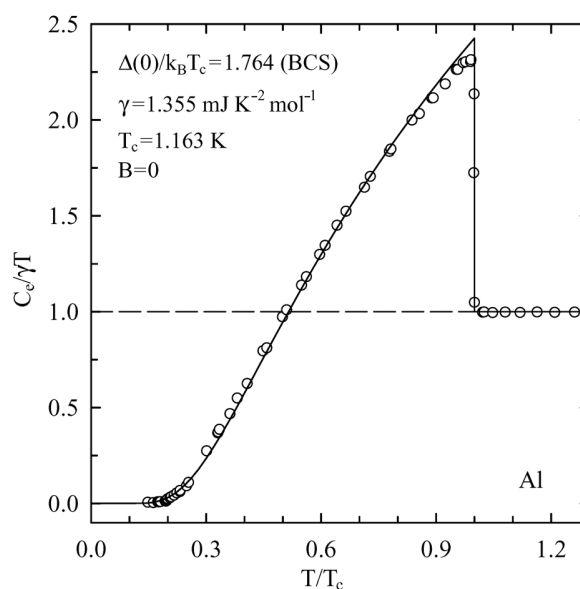

Fig. 1 The zero-field conduction-electron specific heat of Al, in reduced form, $C_e/\gamma T$ *vs.* T/T_c. The solid curve is a fit to the data with the BCS, weak-coupling value of the gap parameter, $\alpha = 1.764$, and other parameters indicated in the figure

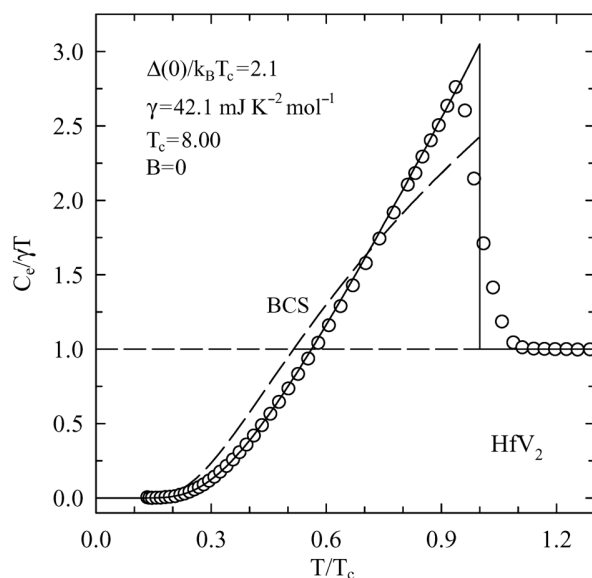[*]   Author for correspondence: nephill@cchem.berkeley.edu

Fig. 2 The zero-field conduction-electron specific heat of HfV$_2$, in reduced form, $C_e/\gamma T$ vs. T/T_c, compared with predictions of the BCS theory in the weak-coupling limit (dashed curve). The solid curve is an α-model, strong-coupling fit, with $\alpha=2.1$

Fig. 3 The zero-field conduction-electron specific heat of MgB$_2$, in reduced form, $C_e/\gamma T$ vs. T/T_c, compared with predictions of the BCS theory in the weak-coupling limit (dashed curve). The solid lines represent a two-gap, α-model fit, and its two components with $\alpha=0.6$ and 2.2

nodes, C_{es} shows the exponential dependence expected for a 'fully gapped' superconductor. In fact, HfV$_2$ is a good example of a strong-coupled superconductor with $\alpha=2.1$, as shown in Fig. 2.

Specific heat of MgB$_2$

The BCS theory of 1957 showed that high values of T_c were favored by small atomic mass [1]. Given the ensuing search for superconductivity in compounds of light elements, including B, and the commercial availability of MgB$_2$ for many years, the late date of the (apparently accidental) discovery [5] of superconductivity in MgB$_2$ was itself a surprise. However, the initial intense interest generated by the discovery derived from the fact that, although the isotope effect [6, 7] suggested that MgB$_2$ was a 'conventional' BCS superconductor with phonon-mediated electron pairing, T_c=39 K seemed too high for that mechanism. The BCS phonon mechanism has been confirmed by theoretical work [8–13], which, in concert with a variety of experimental measurements including heat-capacity measurements, has also shown that MgB$_2$ is an example of multi-gap superconductivity. The possibility of multi-band, multi-gap superconductivity had been recognized theoretically [14] in 1959 and a number of the properties predicted [14, 15–17], but MgB$_2$ is the first example to show the properties so clearly and in such detail. For C_{es} the relevant theoretical predictions for a two-gap superconductor are: 1) for any realistic interband coupling the two gaps will open at
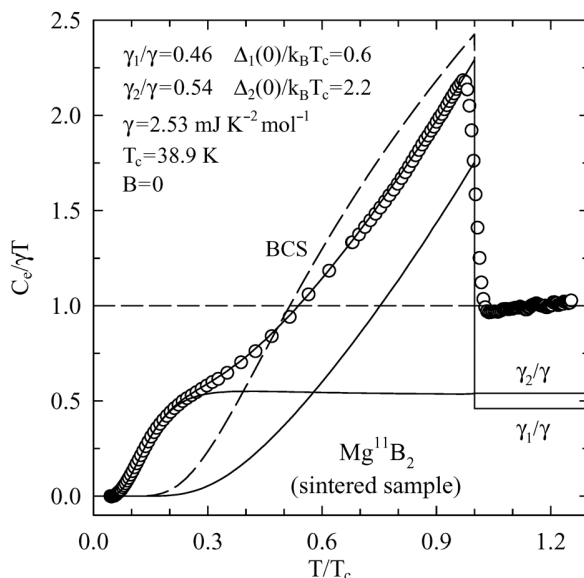
a common T_c; 2) one gap must be smaller than the BCS gap and the other greater; 3) at low temperature C_{es} is determined by the small gap.

Specific heat data were among the earliest experimental evidence of the two-gap nature of the superconductivity of MgB$_2$, and are of particular significance in this context because the specific heat is a bulk property [18–21]. Figure 3 shows comparisons of C_{es} data [21] with a two-gap model [22] and with the BCS theory for the weak-coupling limit. (For this sample T_c=38.9 K and γ=2.53 mJ mol^{-1} K^{-2}.) Below $T_c/2$, $C_{es}/\gamma T$ is greater than the BCS values, by orders of magnitude at the lowest temperatures. This excess contribution shows the presence of excitations at energies below that of the BCS gap, i.e., excitations across the small gap, Δ_1. Near T_c, where the BCS curve has negative curvature, the data show positive curvature, which is characteristic of strong coupling (Fig. 2). However, for strong-coupling superconductors the discontinuity in C_e at T_c is generally greater than the BCS value; in this case it is less. This apparent discrepancy is resolved when there are two gaps on different sheets of the Fermi surface that make additive contributions to C_{es}: The large gap determines the shape of C_{es} near T_c but the magnitude of that contribution is reduced by the fractional contribution of that sheet to γ, γ_2/γ, and the small-gap sheet makes a small, weakly temperature dependent, contribution to C_{es} near T_c. These features in C_{es} are well described by a two-gap, α-model fit [22], as shown in Fig. 3. In Fig. 3, C_{es} is represented as the sum of contributions

from two sheets of the Fermi surface with different values of α, weighed by their fractional contributions to γ, γ_1/γ, and γ_2/γ. (For a single-gap superconductor a value of α less than that of the weak-coupling limit would be physically unrealistic, but for one of the gaps of a two-gap superconductor it is thermodynamically required.) The curve for each contribution makes its role in determining the overall temperature dependence of C_{es} clear. This interpretation of the heat capacity of MgB_2, including the values of the three adjustable parameters, α_1, α_2, and γ_1/γ_2, is in good agreement with a number of spectroscopic measurements [23–27] and theoretical calculations [11–13]. MgB_2 is well established as a two-gap super-conductor, and C_{es} can be taken as a model for comparison with other superconductors that might have more than one gap.

Specific heat of $Na_{0.3}CoO_2\cdot1.3H_2O$

The superconductivity of $Na_{0.3}CoO_2\cdot1.3H_2O$ is of particular interest for comparison with that of the cuprates. The 1986 discovery [28] of superconductivity in the layered perovskite cuprates, for which T_c reaches 133 K [29], raised the question of whether high-T_c superconductivity might be found in similar structures with transition-metal ions other than Cu. Co was recognized as an interesting candidate almost immediately, but the superconductivity of $Na_{0.3}CoO_2\cdot1.3H_2O$, with a relatively low T_c, about 5 K, was not discovered until 2003 [30]. In the cuprates the Cu ions are in corner-sharing O octahedra or pyramids, in an approximately square array. In the parent undoped Mott insulator the Cu ions are ordered antiferromagnetically and antiferromagnetic spin fluctuations are thought to have a role in the electron pairing in the hole-doped superconducting phases. In $Na_{0.3}CoO_2\cdot1.3H_2O$ the Co ions are at the centers of edge-sharing O octahedra, in a triangular array, which produces frustration of the antiferromagnetic interaction that is expected to affect the superconductivity. Theoretical work suggests that the electron pairing in $Na_{0.3}CoO_2\cdot1.3H_2O$ is 'unconventional', and perhaps unique. Experimental work has been limited by the complicated synthetic procedures, the sensitivity of the superconductivity to stoichiometry, and the relative instability of the superconducting material. C_{es} gives information about the symmetry of the gap: For conventional superconductors an exponential decrease of C_{es} corresponds to a fully gapped Fermi surface. For a superconductor with nodes in the gap a power-law temperature dependence is expected, with the exponent determined by the form of the nodes. Point nodes give $C_{es}\propto T^3$; line nodes give $C_{es}\propto T^2$. A
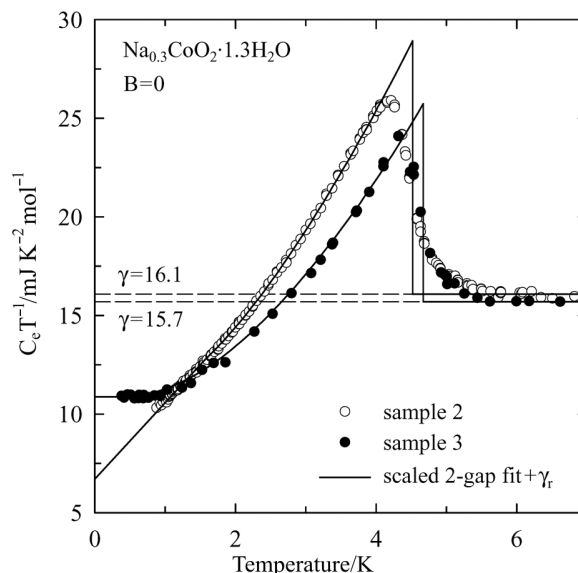

Fig. 4 The zero-field conduction-electron specific heat of two samples of $Na_{0.3}CoO_2\cdot1.3H_2O$ is shown as $C_e/\gamma T$ *vs. T*. The solid curves represent two-gap, α-model fits described in the text, adjusted to correspond to the experimental data as measured

number of heat-capacity measurements have been reported [31–36], but in many cases the interpretation of the data has been limited by substantial contributions from magnetic impurities or a lack of low-temperature data.

Recent measurements of the specific heat of three samples of $Na_{0.3}CoO_2\cdot1.3H_2O$, all prepared in essentially the same way, have given different results [37]. Sample 1 was not superconducting, and the results are not considered here. The results for C_e, for samples 2 and 3 are shown in Fig. 4, as $C_e/\gamma T$ *vs. T*. At the lowest temperatures, sample 2 shows the T^2 behavior characteristic of line nodes in the gap, which has also been reported by Yang *et al.* [36]; sample 3 shows the exponential temperature dependence characteristic of a fully gapped superconductor. Both samples show non-zero intercepts of C_e/T in the limit $T\rightarrow0$, corresponding to 'residual' electron densities of states (DOS), and residual γ's, γ_r. All heat-capacity measurements on this material that permit reasonably unambiguous extrapolations to 0 K show evidence of a contribution of this type. The usual interpretation, is that a fraction of the sample, γ_r/γ, remains normal. The normal-phase fraction is, e.g., 0.51 for another sample [36] that shows a T^2 behavior of C_e, 0.41 for sample 2, and 0.71 for sample 3. On the basis of that interpretation, C_e for one mole of superconducting material is obtained by subtracting γ_r, and scaling the result by γ_r/γ. The results for samples 2 and 3 are shown in Figs 5 and 6.

Above $T/T_c=0.2$ the experimental results for sample 2, and their deviations from BCS theory, are remarkably similar to those for MgB_2, and show that
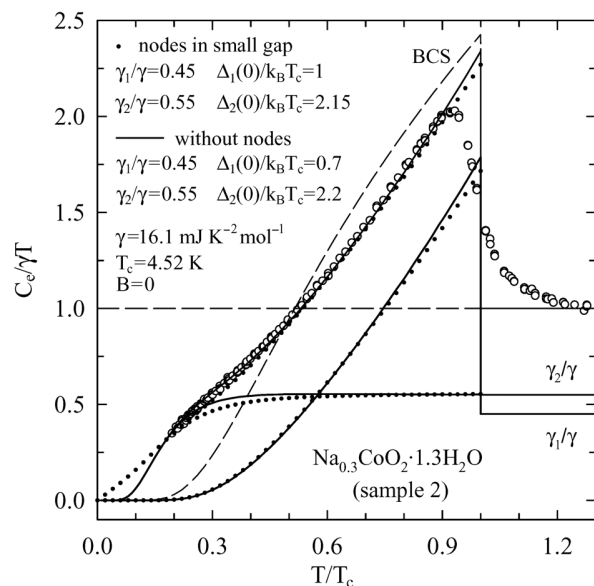
Fig. 5 The zero-field conduction-electron specific heat of Na$_{0.3}$CoO$_2$·1.3H$_2$O, sample 2, in reduced form, $C_e/\gamma T$ vs. T/T_c, compared with predictions of the BCS theory in the weak-coupling limit (dashed curve). The dotted, (solid) curves represent two-gap, α-model fits with, (without) nodes in the small gap, and the parameters indicated in the figure

Fig. 6 The zero-field conduction-electron specific heat of Na$_{0.3}$CoO$_2$·1.3H$_2$O, sample 3, in reduced form, $C_e/\gamma T$ vs. T/T_c, compared with predictions of the BCS theory in the weak-coupling limit (dashed curve). The solid curves represent a two-gap, α-model fit, without nodes, and the parameters indicated in the figure

Na$_{0.3}$CoO$_2$·1.3H$_2$O is another two-gap superconductor. A two-gap fit to the Na$_{0.3}$CoO$_2$·1.3H$_2$O data, similar to that for MgB$_2$ in Fig. 3, but with allowance for the presence of line nodes as suggested by the T^2 behavior, is shown in Fig. 5. The major difference between the fits for Na$_{0.3}$CoO$_2$·1.3H$_2$O and MgB$_2$, which is required by the fact that the α model is based on BCS thermodynamics and cannot represent the effect of nodes in the gap, is that the α-model fit for the small-gap contribution for Na$_{0.3}$CoO$_2$·1.3H$_2$O is made only for $T/T_c \geq 0.4$. At lower temperatures the extension of the small-gap contribution is calculated for line nodes below $T/T_c = 0.4$ is just the difference between the experimental data and the extrapolated large-gap contribution. The small-gap contribution determined in this way is very similar to the contribution of a part of the Fermi surface with a small gap and line nodes in Sr$_2$RuO$_4$ [38]. The results for sample 3 raised the question of whether the data for sample 2 could be fitted without line nodes, and, as shown in Fig. 5, that is the case. With slightly different gap parameters, the data can be represented more-or-less as well, without invoking the presence of nodes. Thus, the data for sample 2 are ambiguous with respect to the existence of nodes: The lowest temperature data give the T^2 behavior, also seen in other measurements [36], which is the signature of line nodes, but the T^2 behavior can be represented as the accidental superposition of contributions from gaps without nodes.

As shown in Fig. 6, the low-temperature behavior of C_{es} for sample 3 is qualitatively different from
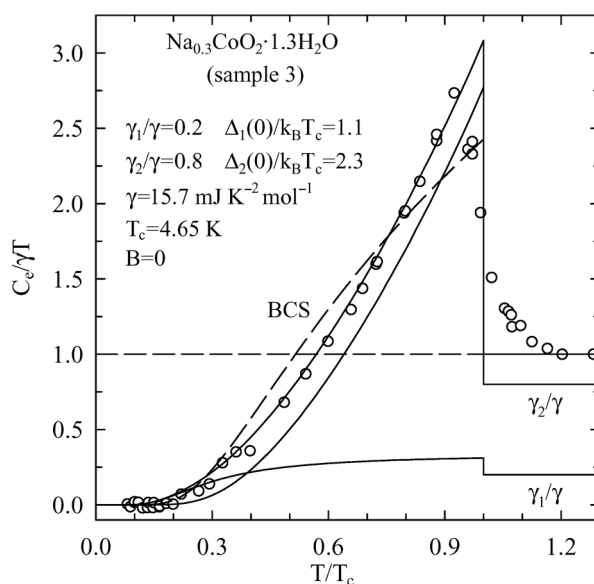
that of sample 2: There is no evidence whatever of T^2 behavior or nodes; the exponential temperature dependence suggests a fully gapped superconductor. The shape of $C_{es}/\gamma T$ still suggests strong coupling, and the data are best fitted by a two-gap model with similar gap parameters, but with a shift in the DOS associated with the small gap to the large gap.

In summary, the results for Na$_{0.3}$CoO$_2$·1.3H$_2$O underline the sensitivity of the properties to sample differences that have not yet been fully identified, possibly subtle differences in ordering of the Na ions or the H$_2$O molecules. They give a clear indication of the presence of two gaps, implying the existence of more than one sheet of the Fermi surface that makes significant contributions to the thermodynamic properties. The evidence for line nodes and unconventional superconductivity for sample 2 is ambiguous, but it seems unlikely that the order parameter is different for the two samples, and the data for sample 3 argue against line nodes. Unusually strong fluctuation effects seen in the specific heat measurements [37], which are not discussed here, do suggest that the nature of the electron pairing is unusual.

Acknowledgements

References

1 J. Bardeen, L. N. Cooper and J. R. Schrieffer, Phys. Rev., 108 (1957) 1175.

2 N. E. Phillips, Phys. Rev., 114 (1959) 676.

3 H. Padamsee, J. E. Neighbor and C. A. Shiffman, J. Low Temp. Phys., 12 (1973) 387.

4 F. R. Drymiotis et al., submitted to Phys. Rev. B.

5 J. Nagamatsu et al., Nature, 410 (2001) 63.

6 S. L. Bud'ko et al., Phys. Rev. Lett., 86 (2001) 1877.

7 D. G. Hinks et al., Nature, 411 (2001) 457.

8 J. M. An and W. E. Pickett, Phys. Rev. Lett., 86 (2001) 4633.

9 J. Kortus et al., Phys. Rev. Lett., 86 (2001) 4656.

10 A. Y. Liu, I. I. Mazin and J. Kortus, Phys. Rev. Lett., 87 (2001) 87005.

11 H. J. Choi et al., Phys. Rev. B, 66 (2002) 20513.

12 H. J. Choi et al., Nature, 418 (2002) 758.

13 A. Golubov et al., J. Phys.: Condens. Matter., 14 (2002) 1353.

14 H. Suhl et al., Phys. Rev. Lett., 3 (1959) 552.

15 B. T. Geilikman et al., Sov. Phys. Solid State, 9 (1967) 642.

16 V. Z. Kresin, J. Low Temp. Phys., 11 (1973) 519.

17 V. Z. Kresin and S. A. Wolf, Physica C, 169 (1990) 476.

18 F. Bouquet et al., Phys. Rev. Lett., 87 (2001) 47001.

19 H. D. Yang et al., 87 (2001) 167003.

20 Y. Wang et al., Physica C, 355 (2001) 179.

21 R. A. Fisher et al., Physica C, 385 (2003) 180.

22 F. Bouquet et al., Europhys. Lett., 56 (2001) 856.

23 F. Giulibeo et al., Phys. Rev. Lett., 87 (2001) 177008.

24 P. Martinez-Samper et al., Physica C, 385 (2003) 233.

25 P. Szabo et al., Phys. Rev. Lett., 87 (2001) 137005.

26 X. K. Chen et al., Phys. Rev. Lett., 87 (2001) 157002.

27 S. Tsuda et al., Phys. Rev. Lett., 87 (2001) 177006.

28 J. G. Bednorz and K. A. Müller, Z. Phys. B, 64 (1986) 189.

29 A. Schilling et al., Nature, 362 (1993) 226.

30 K. Takada et al., Nature, 422 (2003) 53.

31 R. Jin et al., Phys. Rev. Lett., 91 (2003) 217001.

32 G. Cao et al., J. Phys.: Condens. Matter, 15 (2003) L519.

33 B. Lorenz et al., Physica C, 402 (2004) 106.

34 B. G. Ueland et al., Physica C, 402 (2004) 27.

35 F. C. Chou et al., Phys. Rev. Lett., 92 (2004) 157004.

36 H. D. Yang et al., Phys. Rev. B., 71 (2005) 20504.

37 N. Oeschler et al., cond-mat/0409760; accepted for publication in Physica B; accepted for publication in Chinese J. Phys.; to be published.

38 T. Nomura and K.Yamada, J. Phys. Soc. Jpn., 71 (2002) 404.